Association of the *hERG* mutation with long-QT syndrome type 2, syncope and epilepsy

GUOLIANG LI[1*], RUI SHI[1*], JINE WU[1*], WENQI HAN[1], AIFENG ZHANG[2], GONG CHENG[3], XIAOLIN XUE[1] and CHAOFENG SUN[1]

[1]Department of Cardiovascular Medicine, The First Affiliated Hospital of Xi'an Jiaotong University Health Science Center, Xi'an, Shaanxi 710061; [2]Department of Cardiovascular Medicine, The Second Affiliated Hospital of Xi'an Jiaotong University Health Science Center, Xi'an, Shaanxi 710004; [3]Department of Cardiovascular Medicine, Shaanxi Provincial People's Hospital, Xi'an, Shaanxi 710068, P.R. China

Received November 11, 2014; Accepted August 4, 2015

DOI: 10.3892/mmr.2016.4859

Abstract. Mutations in the human ether-à-go-go-related gene (*hERG*) are responsible for long-QT syndrome (LQTS) type 2 (LQT2). In the present study, a heterozygous missense mutation (A561V) linked to LQT2, syncope and epilepsy was identified in the S5/pore region of the hERG protein. The mutation, A561V, was prepared and subcloned into hERG-pcDNA3.0. Mutant plasmids were co-transfected into HEK-293 cells, which stably express wild-type (WT) hERG, in order to mimic a heterozygous genotype, and the whole-cell current was recorded using a patch-clamp technique. Confocal microscopy was performed to evaluate the membrane distribution of the hERG channel protein using a green fluorescent protein tagged to the N-terminus of hERG. A561V-hERG decreased the amplitude of the WT-hERG currents in a concentration-dependent manner. In addition, A561V-hERG resulted in alterations to activation, inactivation and recovery from inactivation in the hERG protein channels. Further evaluation of hERG membrane localization indicated that the A561V-hERG mutant protein was unable to travel to the plasma membrane, which resulted in a trafficking-deficient WT-hERG protein. In conclusion, A561V-hERG exerts a potent dominant-negative effect on WT-hERG channels, resulting in decreased hERG currents and impairment of hERG membrane localization. This may partially elucidate the clinical manifestations of LQTS patients who carry the A561V mutation.

Correspondence to: Dr Chaofeng Sun or Dr Xiaolin Xue, Department of Cardiovascular Medicine, The First Affiliated Hospital of Xi'an Jiaotong University Health Science Center, 277 Yanta West Road, Xi'an, Shaanxi 710061, P.R. China
E-mail: cfsun1@mail.xjtu.edu.cn
E-mail: xxiaolin358@sina.com

*Contributed equally

Key words: mutation, human ether-à-go-go-related gene, long-QT syndrome, whole-cell patch-clamp, trafficking

Introduction

The inherited long-QT syndrome (LQTS) refers to a group of genetic cardiac disorders. LQTS is diagnosed clinically by a prolonged corrected QT (QTc) interval (for males and females, respectively; normal, ≤430 and ≤450 msec, borderline, 431-450 and 451-470 msec, and abnormal, >450 and >470 msec) on a surface electrocardiogram (ECG) (1). This is in addition to abnormal cardiac repolarization resulting in syncope and life-threatening arrhythmias as a consequence of torsades de pointes (TdP) (2,3). TdP is a specific form of polymorphic ventricular tachycardia, often presenting in young healthy individuals, particularly children and teenagers (4-7). Currently, molecular genetic studies have identified hundreds of mutations in ≥13 genes, which are responsible for LQTS, including LQTS type 1 (LQT1) to LQT13 (6). The subtypes LQT1, LQT2 and LQT3 are the most common and account for ~90% of genotype-positive cases worldwide (8,9).

Mutations in the human ether-à-go-go-related gene (*hERG*) are linked to LQT2, which is the most common form of LQTS in China (10,11). The *hERG* is located on human chromosome 7 and encodes the pore-forming α-subunit of the rapidly activating delayed rectifier cardiac potassium current (I_{Kr}), which is a major determinant of cardiac action potential duration in the mammalian heart (12). To date, in patients with LQT2, the majority of mutations in *hERG* increase the transmural dispersion of repolarization and eventually induce prolongation of the QT interval, a notched T wave, re-entry and TdP. Previous functional studies have implicated that various molecular mechanisms are responsible for the non-functional hERG channel (6,7,9). Mutations located in different regions lead to various effects on the biological and electrophysiological consequences of hERG channels; the mechanisms are organized into five categories as follows: Class 1, disruption of Kv11.1 channel synthesis; class 2, protein trafficking; class 3, gating; class 4, permeation; and class 5, degradation of premature termination codon (PTC)-containing mRNA transcripts by nonsense-mediated mRNA decay (13,14).

The current study presents a heterozygous point mutation, 1682C→T in *hERG*, in the individual exhibiting severe clinical manifestations, including LQTS, syncope and epilepsy, often

presenting early in the morning. This mutation leads to substitution of the amino acid, alanine by valine (A561V) in the S5/pore region of the hERG protein. Additionally, stable wild-type (WT) hERG HEK-293 cells were transfected with mutated A561V plasmids, and the expression and function generated by the heterozygous hERG channel was examined to elucidate the clinical manifestations of LQT2 due to the A561V mutation.

Materials and methods

Ethical approval and informed consent. The Ethics Committee of the First Affiliated Hospital of Xi'an Jiaotong University (Xi'an, China) approved the present study. Three patients, including the proband (male; age, 18 years), his mother (53 years) and his father (57 years), were assessed in an outpatient clinic of the First Affiliated Hospital of Xi'an Jiaotong University Health Science Center in August 2013. Written informed consent was obtained from all participants.

Clinical characteristics. The clinical evaluation of the three individuals (the proband and his parents) included a medical and family history check, 12-lead ECG, echocardiography, 24-h Holter recordings and an X-ray of the heart. There was no evidence of structural heart disease, as assessed by echocardiography and the heart X-ray. In addition, none of the participants had a hearing impairment. A prolonged QT interval was diagnosed using a standard 12-lead baseline ECG in the proband (without concomitant therapeutic agent exposure or electrolyte disturbances) according to previously proposed diagnostic criteria (15-17). Bazett's formula (18,19) was used for heart rate correction of the QT interval, with 460 msec for females and 440 msec for males (the two values fall near the upper limits of normal). The control group consisted of 120 unrelated individuals who were randomly selected from a group of healthy Chinese volunteers with no reported cardiovascular history (based on an interview), who exhibited a normal 12-lead ECG.

Mutation of cDNA constructs. A 10-ml sample of whole blood was collected from three of the participant's family members. Genomic DNA was isolated from venous EDTA blood using a DNA Extraction kit obtained from Sangon Biotech Co., Ltd (Shanghai, China). Direct sequencing of the complete coding sequences of the LQTS-associated genes was performed. hERG-A561V was prepared by polymerase chain reaction (PCR) using primers, as follows: Sense, 5'-TTCCTCATC GACATGGTGGC-3' and antisense, 5'-GAGGCTGCTGAA GGTGAAGT-3'. The PCR thermocycling program (Bio-Rad Laboratories, Inc., Hercules, CA, USA) consisted of: 6 min at 95˚C; 30 cycles of 30 sec at 94˚C, 45 sec at 55˚C and 45 sec at 72˚C; 10 min at 72˚C; and 30 min at 4˚C. All primers and materials used in the PCR were obtained from Sangon Biotech Co. Ltd.. The PCR products were verified by sequencing and subcloned into full length hERG-pcDNA3.0.

Cell culture and transfection. Cell culture and transfection were performed as previously described (4) and the transfection efficiency was evaluated using microscopy. Briefly, HEK-293 cells (ICE Bioscience Co., Ltd., Beijing, China) were cultured in high-glucose Dulbecco's modified Eagle's medium (DMEM; Gibco Life Technologies, Carlsbad, CA, USA) containing 10% fetal bovine serum (FBS; Gibco Life Technologies) at 37˚C in an atmosphere of 5% CO_2. The day before transfection, the HEK-293 cells were seeded in 35-mm plastic dishes at a cell density of $2x10^5$ cells/well. In the whole-cell patch-clamp experiment, the A561V vectors were co-transfected into the HEK-293 cells, which stably express WT-hERG, to produce a heterozygous cell phenotype to mimic a heterozygous genotype, as previously described (4). In the patch-clamp experiment using a pcDNA3.0 vector (obtained from Xi'an Jiaotong University), additional 0.5 mg green fluorescent protein (GFP)-pRK5 plasmids (Xi'an Jiaotong University) were co-transfected as a marker of successful transfection. pEGFP-C2-WT and pEGFP-C2-A561V vectors (also from Xi'an Jiaotong University) were transiently transfected into HEK-293 cells for subsequent confocal microscopic analysis. The pDsRed2-ER vector was co-transfected to indicate the endoplasmic reticulum (ER). All transfections were performed according to the manufacturer's instructions [X-tremeGENE™ HP DNA Transfection Reagent (cat. no. 06366236001), Roche Diagnostics GmbH, Mannheim, Germany].

Patch-clamp recordings. Whole-cell patch-clamp recordings were performed to evaluate hERG currents, according to previous protocol (4). Briefly, cells were superfused with a bath solution, which was composed as follows: 140 mM NaCl; 4 mM KCl; 2 mM $CaCl_2$; 1 mM $MgCl_2$; 5 mM glucose; 10 mM 4-(2-hydroxyethyl)-1-piperazineethanesulfonic acid (HEPES); and the pH was adjusted to 7.4 using NaOH. Pipettes were filled with a solution composed as follows: 20 mM KCl; 115 mM K-aspartate; 1 mM $MgCl_2$; 1 mM Na_2ATP; 5 mM ethylene glycol tetraacetic acid; 10 mM HEPES; and the pH was adjusted to 7.2 using KOH. The pipette resistance was 3-5 mΩ. A MultiClamp 700B Amplifier (Molecular Devices, LLP, Sunnyvale, CA, USA) was used to record the membrane currents. No leak subtractions were made and the cell capacitance (in pF) was obtained by whole-cell capacitance compensation. Data were stored and analyzed using pCLAMP 9.2 software (Molecular Devices, LLP). All experiments were conducted at room temperature (22-25˚C).

Expression levels and location of the hERG protein. HEK-293 cells were cultured in 35-mm glass bottom culture dishes (NEST Biotechnology, Vanguard International Investment Co., Ltd., Hong Kong, China) and co-transfected with different plasmids (pDsRed2-ER, pEGFP-C2-WT-hERG or pEGFP-C2-A561V-hERG). The HEK-293 cells were continuously incubated for 48 h at 37˚C and images of the cells were obtained using a FV1000 laser scanning microscope (Olympus Corporation, Tokyo, Japan). The images were analyzed using a FV10-ASW Viewer 4.0 (Olympus Corporation).

Statistical analysis. All values are presented as the mean ± standard error of the mean. Differences among multiple groups were assessed by two-way analysis of variance followed by Dunnett's test. Statistical comparisons between two groups were performed with the two sample t-test and all analyses were performed using SPSS version 18.0 (SPSS, Inc., Chicago, IL, USA). $P<0.05$ was

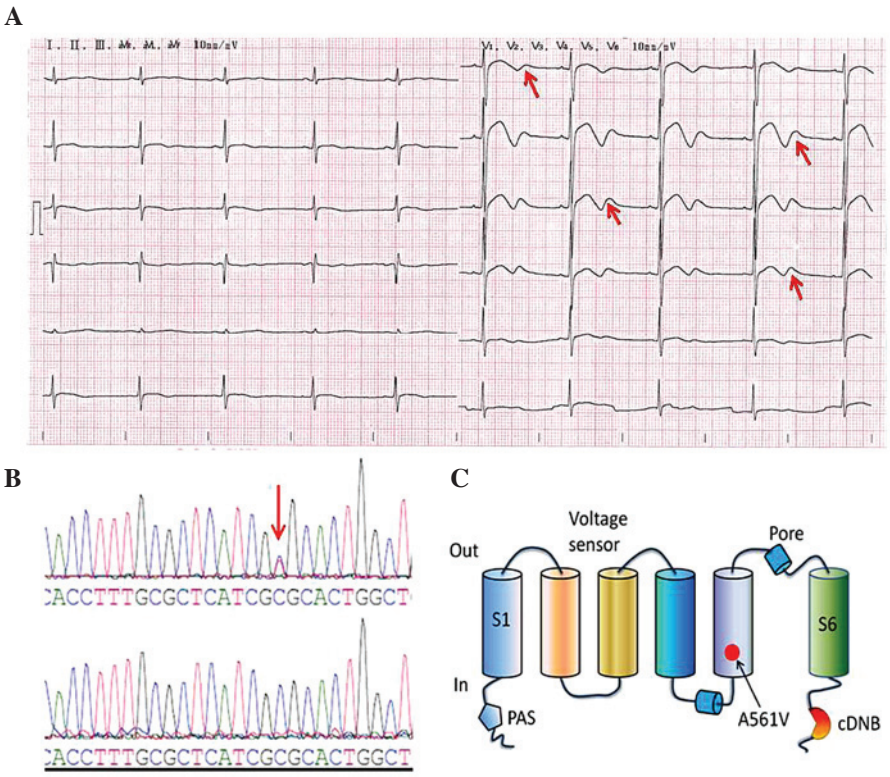

Figure 1. ECG and mutation analysis. (A) ECG of the LQTS patient. The 12-lead ECG revealed a prolonged heart rate-corrected QT interval and biphasic T waves (indicated by the red arrows). (B) DNA sequencing chromatogram demonstrating a heterozygous point mutation, 1682C→T in the *hERG* gene of the LQTS patient (upper DNA sequencing chromatogram) and DNA sequence analysis in a healthy individual (lower DNA sequencing chromatogram); the red arrow indicates the mutation site. (C) This mutation leads to the substitution of the amino acid, alanine (A) by valine (V) in the S5/pore region of the hERG protein (A561V). ECG, electrocardiogram; LQTS, long-QT syndrome; *hERG*, human ether-à-go-go-related gene; cDNB, cyclic-nucleotide-binding domain.

considered to indicate a statistically significant difference. In addition, the voltage-dependence of current activation was determined by fitting the values of the normalized tail currents to a Boltzmann function as follows:

$$I=1/(1+\exp[(V_{1/2}-V_t)/k])$$

Where, I represents the relative tail current; $V_{1/2}$, the voltage at which the current is half activated; V_t, the test potential; and k, the slope factor. The time-dependence of current activation was determined by fitting the values of the normalized tail currents to a single exponential function as follows:

$$I=I_0+A\exp(-x/\tau),$$

Where, I represents the relative tail current; I_0, the residual current, which is unfitted; and τ, the time constant. The association between the dose of the plasmid, PC-DNA3.0-A561V-hERG and the current was determined by fitting values to a Hill equation, following normalization of the post-transfection currents to the control currents without A561V transfection, as follows:

$$I=1/[1+(IC_{50}/D)^n],$$

Where, I represents the relative tail current; $IC_{50,}$ the concentration required for 50% channel blockade; D, the A561V plasmid dose for transfection; and n, the Hill coefficient.

Results

Patient was clinically characterized with LQT2 due to A561V mutation. The proband had presented with the main symptom of frequent episodes of syncope during physical or emotional stress over the past 13 years. A 12-lead ECG demonstrated a prolonged QTc interval and biphasic T waves (Fig. 1A), indicating a genetic defect in the *hERG* gene, which is linked to LQT2. Echocardiography and an X-ray did not reveal any structural cardiac disease in the patient. Additionally, there was no evidence of exposure to therapeutic agents or electrolyte disturbances. As shown in Fig. 1B-C, the initial genetic screening revealed a heterozygous cytosine to thymine nucleotide exchange in the *hERG* gene in the proband, but not in the other family members, leading to the substitution of alanine by valine at amino acid position 561 (A561V) in the S5/pore region of the hERG protein. This mutation was not observed in the 120 healthy control individuals.

A561V exerts a dominant-negative effect on the hERG channels. To define the functional change of the A561V mutation, A561V channels were transiently transfected into HEK-293 cells stably expressing WT-hERG. I_{Kr} was elicited by the protocol demonstrated in Fig. 2Aa (a standard protocol used to investigate hERG) (4). Briefly, the holding potential was maintained at -80 mV, and tail currents were recorded at a level of -40 mV for 4 sec following depolarizing pulses from -60 to +60 mV in 10-mV increments for 2 sec. No current was detected

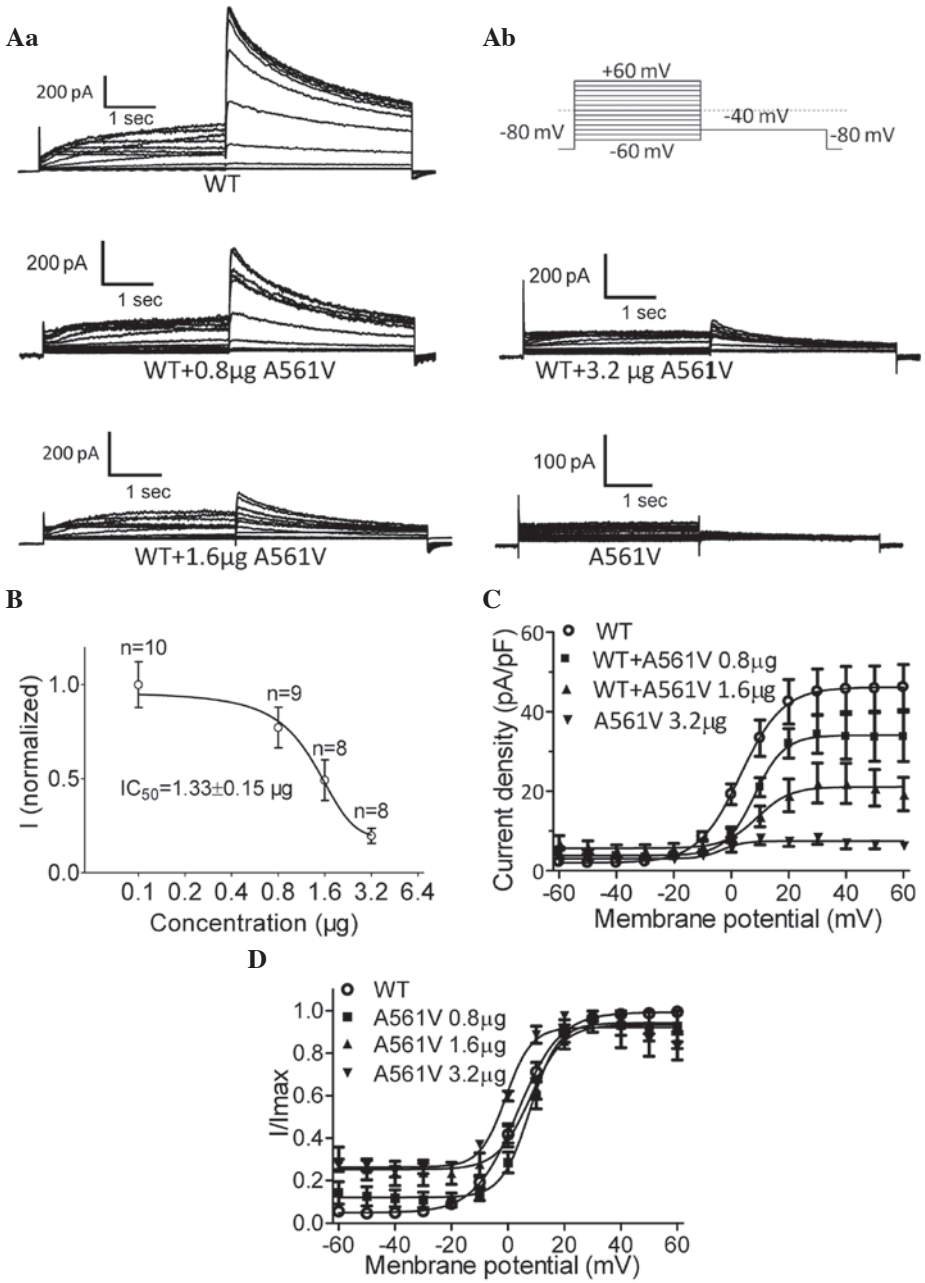

Figure 2. A561V mutation dose-dependently suppressed the currents in HEK-293 cells stably expressing WT-hERG. (Aa) Representative whole-cell current traces obtained from cells stably expressing WT-hERG with and without varying quantities of A561V-hERG plasmid (0.8, 1.6 and 3.2 μg), as well as the currents in cells exhibiting the A561V mutation. (Ab) A portion of the voltage-clamp protocol. (B) Dose-dependent inhibition of hERG currents by the A561V mutation. (C) I-V associations of the tail currents obtained from WT-hERG cells and A561V-hERG plasmid-transfected WT-hERG cells. (D) The I-V curves were normalized to a Boltzmann function. WT, wild-type; hERG, human ether-à-go-go-related gene; I, current; V, voltage.

in the cells that were transiently expressing homozygous A561V channels. In the co-expression experiments, A561V dose-dependently decreased WT-hERG currents. Fig. 2b demonstrates representative whole-cell current traces obtained from cells stably expressing WT-hERG with and without varying quantities of the A561V-hERG plasmid. The maximum attainable WT-hERG tail current density was 46.2±2.0 pA/pF. By contrast, following transfection of 0.8-, 1.6- and 3.2-μg A561V-hERG plasmids, the current densities were 34.1±1.6, 21.1±1.6 and 7.5±0.5 pA/pF, respectively. Transfection of the A561V-hERG plasmid dose-dependently inhibited the hERG current in cells stably expressing WT-hERG (Fig. 2B), with an IC_{50} of 1.33±0.15 μg. The association between the current (I) and voltage (V) of the tail currents obtained from the WT-hERG cells and the A561V-hERG plasmid-transfected WT-hERG cells is shown in Fig. 2C. These results indicate that A561V-hERG exerts a dominant-negative effect on the WT-hERG channels. Additionally, HEK-293 cells transfected with A561V plasmids did not exhibit any hERG-like currents, indicating that homozygous A561V-hERG does not produce functional hERG channels.

The normalized tail currents of WT-hERG were plotted as a function of the test potential and were then fitted to a Boltzmann function, as previously described (4). As shown in Fig. 2D, the voltage to achieve half activation ($V_{1/2}$) for the WT-hERG was 3.34±0.57 mV compared with $V_{1/2}$ values

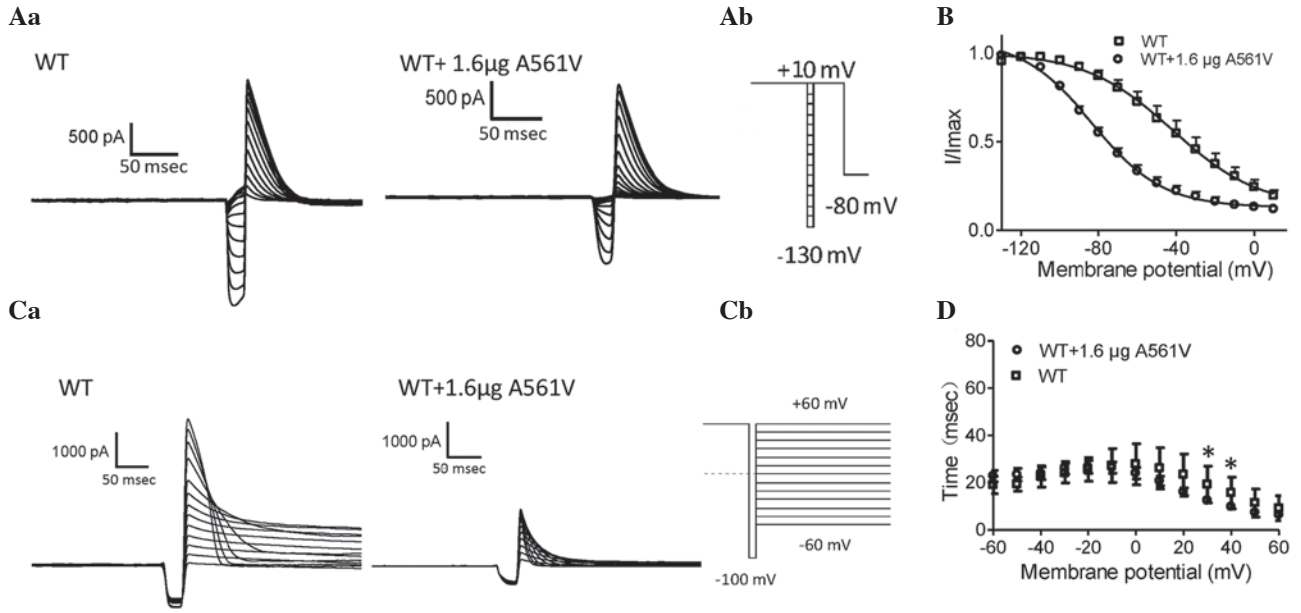

Figure 3. Steady-state inactivation and time courses of inactivation analysis. (Aa) Representative steady-state inactivation current traces. (Ab) A portion of the voltage-clamp protocol. (B) Normalized steady-state inactivation curves for WT-hERG and 1.6-μg A561V-transfected WT-hERG cells, respectively. (Ca) Representative current traces of the time courses of inactivation and inactivation time constant values (τ) for WT-hERG and 1.6-μg A561V-transfected WT-hERG cells. (Cb) A portion of the voltage-clamp protocol. (D) Normalized inactivation time constant, τ, in cells expressing WT-hERG and 1.6-μg A561V-transfected WT-hERG cells. τ was measured by fitting the inactivating currents, during test pulses at each potential, with a single exponential function. *P<0.05, WT vs. A561V-transfected WT group. WT, wild-type; hERG, human ether-à-go-go-related gene; I, current; V, voltage.

of 7.77±1.07, 7.97±1.48 and -0.77±0.90 mV for WT-hERG cells transfected with 0.8, 1.6 and 3.2 μg A561V plasmids, respectively. Significant differences were observed between the WT-hERG cells and all of the A561V-transfected groups; the slope factor, k, in the WT-hERG and 0.8-, 1.6- and 3.2-μg A561V-hERG transfected cells was 7.59±0.50, 4.97±0.94, 5.81±1.29 and 4.57±0.84, respectively (Fig. 2D). Thus, A561V-hERG may alter the voltage dependence of hERG activation.

To analyze steady-state inactivation, test potentials between -130 and 10 mV in 10-mV increments for 20 msec were applied following a depolarizing pulse to 10 mV for 4 sec. This was followed by a test pulse returning to 10 mV for 500 msec prior to a final return of the voltage to the holding potential of -80 mV. The protocol is shown in Fig. 3Aa and is a standard protocol adopted to evaluate hERG channels (4). Representative steady-state inactivation current traces for WT-hERG and 1.6-μg A561V-transfected WT-hERG were obtained from HEK-293 cells (Fig. 3A). Fig. 3B demonstrates the resulting normalized steady-state inactivation curves. The voltages to achieve $V_{1/2}$ were -41.9±5.0 and -83.4±1.95 mV for WT-hERG and 1.6-μg A561V-transfected WT-hERG cells, respectively; a negative shift of ~41 mV, respectively. The k values were -22.3±4.86 for WT-hERG and -18.26±1.69 for 1.6-μg A561V-transfected WT-hERG. These results indicate that A561V-hERG alters the inactivation gating of the WT-hERG channel.

The course of inactivation of hERG channels over time was measured according to the previously described protocol (4). Briefly, a three pulse protocol was used as follows: The pulse comprises a holding potential of -80 mV and a 2-sec pulse to +60 mV to activate and inactivate the hERG channels, followed by a hyperpolarized pulse to -100 mV for 10 msec to recover from inactivation. In the third pulse, a varied test pulse between -60 and +60 mV in 10-mV increments was allowed to elicit inactivating currents. Representative traces of inactivation currents were obtained from WT-hERG cells and WT-hERG cells transfected with 1.6 μg A561V-hERG (Fig. 3C). The currents elicited by the third pulses were then fitted with a single exponential function and plotted as a function of test potential to estimate the time constants of inactivation (Fig. 3D). The time course of inactivation in cells expressing WT-hERG with A561V was observed to be shorter than those cells without A561V only at 30 and 40 mV. This indicates that A561V-hERG facilitates hERG channel inactivation.

Recovery from inactivation was measured according to a previously described protocol (4). Briefly, the holding potential was at -80 mV and then depolarized to 60 mV for 1.5 sec in order to activate and inactivate the channels. Repolarization occurred from -120 to -20 mV at 10-mV increments. The channels recovered from inactivation at the repolarization potential, which was fitted to a single exponential function. Representative current traces were obtained from WT-hERG and A561V-transfected WT-hERG cells (Fig. 4A). Fig. 4B demonstrates the time constant value (τ) of recovery from inactivation. There are significant differences only at -110 mV, where the recovery from inactivation in WT-hERG cells is faster than that of the heterozygotes (P<0.05).

Deactivation was measured according to the same protocol as inactivation. Fig. 4C demonstrates the representative current recordings of WT-hERG and A561V-transfected WT-hERG cells. Fig. 4D and E demonstrate fast and slow deactivation, and no significant difference was observed between the two groups for fast and slow deactivation. These findings indicate that A561V-hERG does not affect the deactivation of the WT-hERG channels.

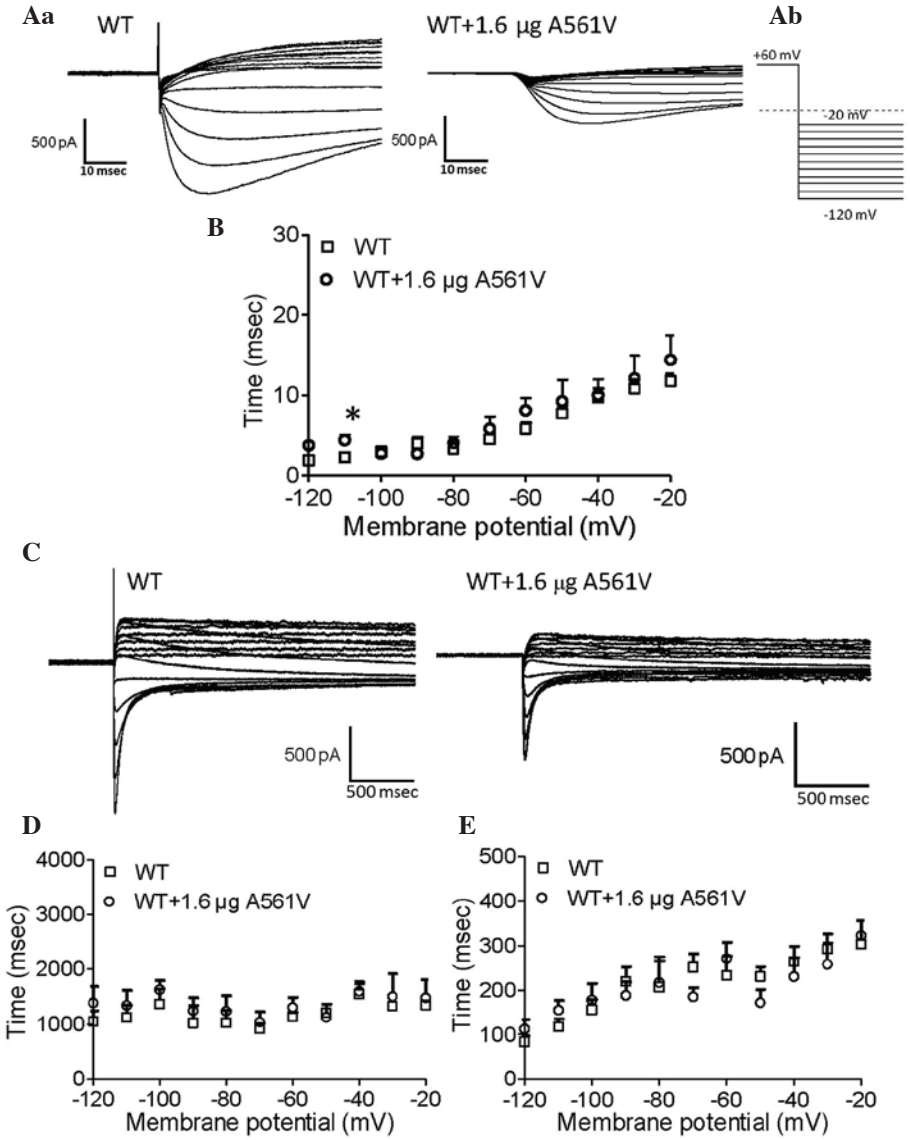

Figure 4. Kinetics of recovery from inactivation and deactivation analysis. (Aa) Representative current traces showing recovery from inactivation were obtained from WT-hERG and 1.6-μg A561V-transfected WT-hERG cells. (Ab) A portion of the voltage-clamp protocol. (B) Time constant (τ) values of recovery from inactivation for WT-hERG and 1.6-μg A561V-transfected WT-hERG cells. (C) Representative current recordings of deactivation in WT-hERG and 1.6-μg A561V-transfected WT-hERG cells. (D) Fast and (E) slow deactivation components of deactivation time constants (τ) as a function of test potential in WT-hERG and 1.6-μg A561V-transfected WT-hERG cells. *P<0.05, WT vs. A561V-transfected WT group. WT, wild-type; hERG, human ether-à-go-go-related gene; I, current; V, voltage.

A561V mutant channels are retained and lead to dysfunctional trafficking. To refine the molecular mechanism of the mutation, A561V-hERG and assess whether the mutation impedes the subcellular localization of the channels, each vector was tagged with green fluorescent protein (pEGFP) and subsequently co-transfected with pDsRed2-ER (red) into the HEK-293 cells (Fig. 5). Following transfection (at 48 h), cells were observed by confocal laser scanning microscopy. As shown in Fig. 5, the left, central and right columns represent the pEGFP, pDsRed2-ER and merged images, respectively. The pEGFP-C2-WT protein (top panel) was predominantly identified on the cell surface, indicating normal trafficking of this protein from the ER to the plasma membrane, as previously described (3,5,7). By contrast, the subcellular localization of the pEGFP-C2-A561V protein was markedly disturbed in the cytoplasm (Fig. 5; middle panel). The pEGFP-C2-WT and pEGFP-C2-A561V proteins were co-expressed in the cytoplasm and on the cell surface (Fig. 5; bottom panel). These observations indicate that A561V mutant channels are retained in the ER, which leads to dysfunctional trafficking.

Discussion

The underlying mechanisms of LQT2 have previously been identified, and include disruption of Kv11.1 channel synthesis, protein trafficking, gating or permeation and degradation of PTC-containing mRNA transcripts by nonsense-mediated mRNA decay (13,14). The majority of LQT2 mutations reduce hERG currents by the trafficking-deficient mechanism (4,5,20). In the present study, a gene mutation, A561V-hERG, was screened for based on

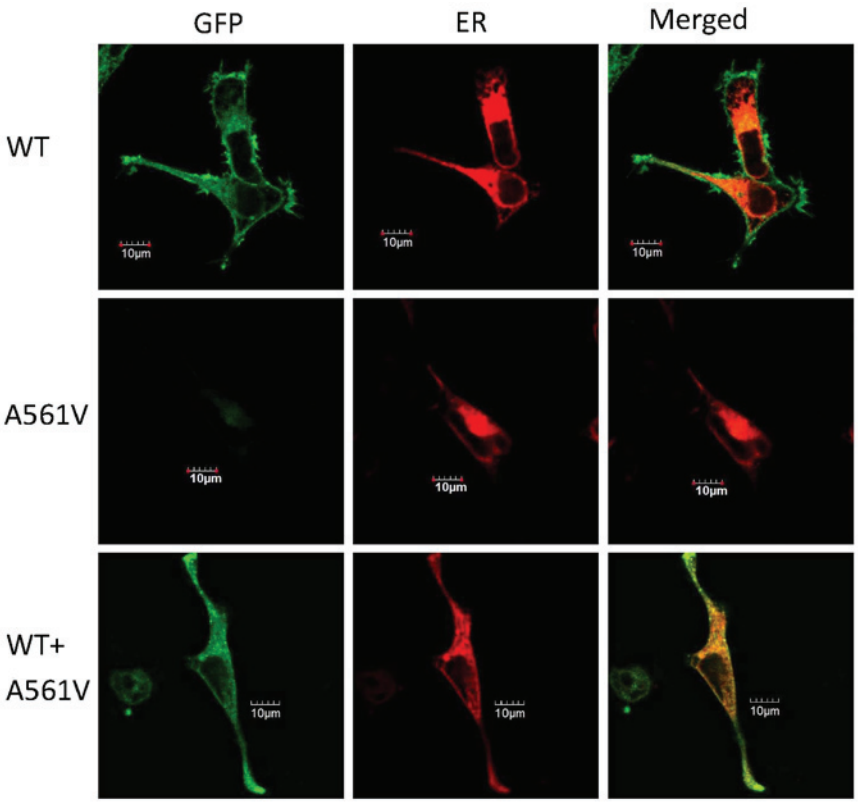

Figure 5. Representative images of subcellular localization of the hERG protein expressed in HEK-293 cells. Top panel, HEK-293 cells expressing pEGFP-C2-WT; middle panel, HEK-293 cells expressing pEGFP-C2-A561V; and bottom panel, HEK-293 cells expressing pEGFP-C2-WT and pEGFP-C2-A561V. Left column, the hERG protein tagged with green fluorescence (green); middle column, HEK-293 cells transfected with pDsRed2-ER (red); and right column, merge of the two. Scale bar, 10 μm. GFP, green fluorescent protein; ER, endoplasmic reticulum, WT, wild-type.

the typical ECG morphology consistent with LOT2 in the sporadic case of an individual who exhibited severe clinical manifestations, including TdP, syncope and epilepsy. The result of the screening verified our clinical diagnosis. This mutation affects an alanine at amino acid position 561 in the S5/pore region of the hERG protein. It is hypothesized that the A561V-hERG mutant protein travels to the plasma membrane and fails to generate any functioning hERG currents in homozygous cells. The A561V-hERG protein has a dominant-negative effect on the WT-hERG protein, resulting in decreased hERG currents and this may be responsible for a prolonged QT interval as observed by ECG.

Previous studies have demonstrated that there are distinct risk factors that provide phenotypic clues associated with the different LQTS genotypes (21,22). In certain cases, the clinical presentation indicates the affected channel genes. For example, carriers of the *KCNQ1* mutation (LQT1) are more prone to syncope during exercise (23), such as swimming (24), whereas those carrying the *hERG* mutation (LQT2) often experience attacks in the early morning, which are frequently elicited by loud noises, such as sirens and alarm clocks (21,25). Carriers of the *SCN5A* mutation (LQT3) experience the majority of their cardiac events during sleep (25). In the current study, the patient had a history of self-terminating ventricular tachycardia, and the majority of the syncopal episodes were in the morning. Based on the occurrence of cardiac events and the pattern of syncopal episodes, it was concluded that the affected individual exhibited characteristics of LQT2 or LQT3.

Genotype identification by ECG is useful for stratifying molecular genetic studies. Previous studies reported an association of certain genotype-specific T wave patterns with LQT1, LQT2 and LQT3 (22,23,26). Typical ST-T wave patterns are present in the majority of genotyped LQTS patients, and may be used to identify LQT1, LQT2 and potentially the LQT3 genotypes. ECG analysis may improve genotype identification accuracy and simplify genetic screening by targeting the gene for initial investigation. The multiple ST-T patterns in each genotype cause uncertainty with regard to the pathophysiology and regulation of repolarization in LQTS (22). LQT1 and LQT2 account for 87% of all patients genotyped to date, and typical ECG patterns were observed in 88% of patients with the LQT1 and LQT2 carriers (27,28). LQT1 patients exhibit broad-based T waves with rather large amplitudes; this is in contrast to LQT2 patients, who exhibit low-amplitude T waves. Furthermore, bifid T waves are considered to be a hallmark of the LQT2 genotype (22,29). The ECG characteristics of LQT3 patients include the late onset of peaked, bifid or asymmetrical T waves. In the current study, the proband demonstrated the same LQT2 bifid T wave that is associated with a history of syncope. This hypothesis supported the finding of the A561V mutation, which was identified by screening *hERG* as the preferred candidate gene.

To determine the effects of A561V-hERG on the hERG currents in heterozygotes, A561V-hERG plasmids were transiently transfected into HEK-293 cells stably expressing WT-hERG, as previously described (4). In this model, the

expression of the WT-hERG channel in cells was increasingly homogeneous when compared with that of the subsequent transient transfection of WT-hERG cells, and served as an ideal model in which to investigate the effects of varying concentrations of A561V-hERG plasmids on hERG currents. A561V-hERG plasmid-transfection was shown to dose-dependently reduce the tail currents in cells expressing WT-hERG channels (IC_{50}, 1.33±0.15 μg). Additionally, the present study demonstrates that the transiently transfected mutant channels did not result in any currents.

Mutations may lead to loss of function of the hERG channels, potentially resulting in haploinsufficiency or dominant-negative suppression of WT-hERG channels (4,5,20,30,31). At the cellular level, loss of function is represented by non- or malfunctioning channels inserted into the plasma membrane (30,32), or by mutant channels retained in the ER due to structural defects (4,5,7). Our previous study reported that one G604S-hERG mutation in the S5/pore region of the hERG protein did not express any functional ion current, and this effect has been attributed to protein trafficking-deficient mechanism, which reduced surface expression of the protein (7). Certain mutant proteins cause dominant-negative suppression of WT-hERG (4,5,7). When co-assembled with WT-hERG proteins, these toxic proteins reduce channel function by >50%. L539fs/47, a truncated mutation at the C-terminus of hERG channels, forms a tetramer with the WT-hERG proteins, causing defective trafficking of WT and mutant proteins and inducing a >50% loss of channel function (4).

S5, S6 and the intervening P-loop form the pores of the ion channel; however, in the homozygous mutant located in the S5/pore region of the hERG protein, it is possible that the A561V-hERG proteins fail to transfer to the cell membrane and cannot create functional channels. This was validated in the present study by patch-clamp experiments in which no currents were recorded in the HEK-293 cells that were transiently transfected with A561V. A number of LQT2 mutations have been shown to be functionally dominant when co-expressed. Zhou *et al* (30) revealed that homo-tetramers of certain LQT2 mutants are abnormally processed when expressed in mammalian cells, and result in instability and retention of the channel protein within intracellular compartments (30,33). However, other mutant proteins do not exhibit dominant-negative suppression of WT-hERG. They cannot co-assemble with WT-hERG proteins to form heterotetramers. By this method, the WT-hERG protein forms a homotetramer and loses 50% of channel function (14,32,34,35).

In the present study, A561V reduced normal hERG currents and the mutant protein exerted a dominant-negative effect by suppressing the WT-hERG protein. The mutation appears to be clinically malignant, as the proband had suffered severe clinical manifestations, including LQTS and syncope over the past 13 years. The functional data indicate that A561V exerts the same protein trafficking-deficient mechanisms as F463L-hERG and G604S-hERG mutations that have previously been described (5,7). A possible interpretation is that severe space constraints in the S5/pore region of the hERG protein during folding and assembly do not tolerate this exchange of amino acids (5).

To analyze the gating properties of the heterozygous channels, the kinetics of the heterozygous channel were compared with those in the WT-hERG cells. Overexpression of A561V-hERG altered the gating properties of WT-hERG channels, including activation, inactivation and recovery from inactivation. A561V-hERG enhanced the steady-state inactivation of hERG channels and altered the $V_{1/2}$ of hERG channels. Inactivation of the heterozygous cells expressing WT-hERG and A561V-hERG channels became accelerated when compared with cells expressing WT-hERG channels at certain potentials (+30 and +40 mV). Similar results were observed in the F463L-hERG, G604S-hERG and a truncated mutation, L539fs/47-hERG, which were previously reported upon (4).

Fluorescence microscopy experiments did not reveal any staining of the A561V-hERG mutant on the plasma membrane, which is in accordance with the absence of I_{Kr}. Co-staining with an ER marker indicated that the A561V-hERG mutant subunit was trapped in the ER and, thus, the channel trafficking was significantly disrupted. Further analysis revealed that co-expression of the mutant protein was detected on the cell membrane; however, it was weaker than the expression of WT-hERG protein alone. These results indicate that A561V-hERG decreases the expression of the WT-hERG protein and reduces the currents of the WT-hERG channels (31). By inference, it is proposed that A561V may co-assemble as a tetramer with WT-hERG to form a heterozygous hERG channel.

LQT2 patients exhibiting mutations in the pore region (amino acid residues 550-650) of the hERG protein are at a markedly increased risk for arrhythmia-associated cardiac events, when compared with patients with non-pore mutations (25). These patients exhibit severe clinical manifestations of the genetic disorder and experience a higher frequency of arrhythmia-associated cardiac events. Furthermore, LQT2 patients experience their first cardiac event at a younger age. This increased risk associated with pore mutations persists throughout the first 40 years of life (25). In the Chinese patient presenting with LQTS in the current study, the mutation was located in the S5/pore region, with the patient exhibiting a prolonged QTc on the ECG, as well as experiencing syncopal episodes. The symptoms of the patient had appeared over the past 13 years, indicating that this S5/pore region mutation (A561V-hERG) is associated with a high risk for developing lethal arrhythmias.

In conclusion, an A561V-hERG mutation in the S5/pore region was screened based on the typical ECG morphology and clinical features of LQT2 and syncopal episodes. The A561V-hERG mutant protein was unable to travel to the plasma membrane and failed to generate functioning hERG currents in homozygous cells. In addition, the A561V-hERG mutant protein exerted a dominant-negative effect on the WT-hERG channels, resulting in decreased hERG currents. This may partly elucidate the clinical manifestations exhibited by the individual carrying the mutation.

Acknowledgements

The present study was supported by the National Natural Science Foundation of China (grant nos. 81400258 and 81270236). Xi'an Jiaotong University Graduate Independent Innovation Research

(grant no. CX1116). The authors would like to thank Dr. Yingji Li for contributions to the statistical analysis.

References

1. Li G, Cheng G, Wu J, Zhou X, Liu P and Sun C: Drug-induced long QT syndrome in women. Adv Ther 30: 793-802, 2013.
2. Liu L, Hayashi K, Kaneda T, Ino H, Fujino N, Uchiyama K, Konno T, Tsuda T, Kawashiri MA, Ueda K, *et al*: A novel mutation in the transmembrane nonpore region of the KCNH2 gene causes severe clinical manifestations of long QT syndrome. Heart Rhythm 10: 61-67, 2013.
3. Nakano Y and Shimizu W: Genetics of long-QT syndrome. J Hum Genet: Jun 25, 2015 (Epub ahead of print).
4. Zhang A, Sun C, Zhang L, Lv Y, Xue X, Li G, Cui C and Yan GX: L539 fs/47, a truncated mutation of human ether-a-go-go-related gene (hERG), decreases hERG ion channel currents in HEK 293 cells. Clin Exp Pharmacol Physiol 40: 28-36, 2013.
5. Yang HT, Sun CF, Cui CC, Xue XL, Zhang AF, Li HB, Wang DQ and Shu J: HERG-F463L potassium channels linked to long QT syndrome reduce I(Kr) current by a trafficking-deficient mechanism. Clin Exp Pharmacol Physiol 36: 822-827, 2009.
6. Bokil NJ, Baisden JM, Radford DJ and Summers KM: Molecular genetics of long QT syndrome. Mol Genet Metab 101: 1-8, 2010.
7. Huo J, Zhang Y, Huang N, Liu P, Huang C, Guo X, Jiang W, Zhou N, Grace A, Huang CL and Ma A: The G604S-hERG mutation alters the biophysical properties and exerts a dominant-negative effect on expression of hERG channels in HEK293 cells. Pflugers Arch 456: 917-928, 2008.
8. Ackerman MJ: Cardiac causes of sudden unexpected death in children and their relationship to seizures and syncope: Genetic testing for cardiac electropathies. Semin Pediatr Neurol 12: 52-58, 2005.
9. Napolitano C, Priori SG, Schwartz PJ, Bloise R, Ronchetti E, Nastoli J, Bottelli G, Cerrone M and Leonardi S: Genetic testing in the long QT syndrome: Development and validation of an efficient approach to genotyping in clinical practice. Jama 294: 2975-2980, 2005.
10. Li C and Liu W: Research status of genetic screening and molecular mechanisms of long QT syndrome in China. Chinese Journal of Cardiac Pacing and Electrophysiology 39: 397-399, 2011 (In Chinese).
11. Chinese Society of Cardiology: Chinese expert consensus on inherited cardiac ion channel disease and cardiomyopathy gene testings. Chinese Journal of Cardiology 39: 1073-1082, 2011. (In Chinese).
12. Sanguinetti MC and Tristani-Firouzi M: hERG potassium channels and cardiac arrhythmia. Nature 440: 463-469, 2006.
13. Delisle BP, Anson BD, Rajamani S and January CT: Biology of cardiac arrhythmias: Ion channel protein trafficking. Circ Res 94: 1418-1428, 2004.
14. Gong Q, Zhang L, Vincent GM, Horne BD and Zhou Z: Nonsense mutations in hERG cause a decrease in mutant mRNA transcripts by nonsense-mediated mRNA decay in human long-QT syndrome. Circulation 116: 17-24, 2007.
15. Kirchhof P, Franz MR, Bardai A and Wilde AM: Giant T-U waves precede torsades de pointes in long QT syndrome: A systematic electrocardiographic analysis in patients with acquired and congenital QT prolongation. J Am Coll Cardiol 54: 143-149, 2009.
16. Morita H, Wu J and Zipes DP: The QT syndromes: Long and short. Lancet 372: 750-763, 2008.
17. Levine E, Rosero SZ, Budzikowski AS, Moss AJ, Zareba W and Daubert JP: Congenital long QT syndrome: Considerations for primary care physicians. Cleve Clin J Med 75: 591-600, 2008.
18. Luo S, Michler K, Johnston P and Macfarlane PW: A comparison of commonly used QT correction formulae: The effect of heart rate on the QTc of normal ECGs. J Electrocardiol 37: 81-90, 2004.
19. Chiladakis J, Kalogeropoulos A, Zagkli F, Koutsogiannis N, Chouchoulis K and Alexopoulos D: Predicting torsade de pointes in acquired long QT syndrome: Optimal identification of critical QT interval prolongation. Cardiology 122: 3-11, 2012.
20. Anderson CL, Delisle BP, Anson BD, Kilby JA, Will ML, Tester DJ, Gong Q, Zhou Z, Ackerman MJ and January CT: Most LQT2 mutations reduce Kv11.1 (hERG) current by a class 2 (trafficking-deficient) mechanism. Circulation 113: 365-373, 2006.
21. Zhang Y, Zhou N, Jiang W, Peng J, Wan H, Huang C, Xie Z, Huang CL, Grace AA and Ma A: A missense mutation (G604S) in the S5/pore region of HERG causes long QT syndrome in a Chinese family with a high incidence of sudden unexpected death. Eur J Pediatr 166: 927-933, 2007.
22. Zhang L, Timothy KW, Vincent GM, Lehmann MH, Fox J, Giuli LC, Shen J, Splawski I, Priori SG, Compton SJ, *et al*: Spectrum of ST-T-wave patterns and repolarization parameters in congenital long-QT syndrome: ECG findings identify genotypes. Circulation 102: 2849-2855, 2000.
23. Moss AJ, Schwartz PJ, Crampton RS, Tzivoni D, Locati EH, MacCluer J, Hall WJ, Weitkamp L, Vincent GM, Garson A Jr, *et al*: The long QT syndrome. Prospective longitudinal-study of 328 families. Circulation 84: 1136-1144, 1991.
24. Moss AJ, Robinson JL, Gessman L, Gillespie R, Zareba W, Schwartz PJ, Vincent GM, Benhorin J, Heilbron EL, Towbin JA, *et al*: Comparison of clinical and genetic variables of cardiac events associated with loud noise versus swimming among subjects with the long QT syndrome. Am J Cardiol 84: 876-879, 1999.
25. Schwartz PJ, Priori SG, Spazzolini C, Moss AJ, Vincent GM, Napolitano C, Denjoy I, Guicheney P, Breithardt G, Keating MT, *et al*: Genotype-phenotype correlation in the long-QT syndrome: Gene-specific triggers for life-threatening arrhythmias. Circulation 103: 89-95, 2001.
26. Dausse E, Berthet M, Denjoy I, André-Fouet X, Cruaud C, Bennaceur M, Fauré S, Coumel P, Schwartz K and Guicheney P: A mutation in HERG associated with notched T waves in long QT syndrome. J Mol Cell Cardiol 28: 1609-1615, 1996.
27. Moss AJ, Zareba W, Kaufman ES, Gartman E, Peterson DR, Benhorin J, Towbin JA, Keating MT, Priori SG, Schwartz PJ, *et al*: Increased risk of arrhythmic events in long-QT syndrome with mutations in the pore region of the human ether-a-go-go-related gene potassium channel. Circulation 105: 794-799, 2002.
28. Splawski I, Shen JX, Timothy KW, Lehmann MH, Priori S, Robinson JL, Moss AJ, Schwartz PJ, Towbin JA, Vincent GM and Keating MT: Spectrum of mutations in long-QT syndrome genes KVLQT1, HERG, SCN5A, KCNE1 and KCNE2. Circulation 102: 1178-1185, 2000.
29. Jongbloed RJ, Wilde AA, Geelen JL, Doevendans P, Schaap C, Van Langen I, van Tintelen JP, Cobben JM, Beaufort-Krol GC, Geraedts JP and Smeets HJ: Novel KCNQ1 and HERG missense mutations in Dutch long-QT families. Hum Mutat 13: 301-310, 1999.
30. Zhou ZF, Gong QM, Epstein ML and January CT: HERG channel dysfunction in human long QT syndrome: Intracellular transport and functional defects. J Biol Chem 273: 21061-21066, 1998.
31. Kagan A, Yu ZH, Fishman GI and McDonald TV: The dominant negative LQT2 mutation A561V reduces wild-type HERG expression. J Biol Chem 275: 11241-11248, 2000.
32. Sanguinetti MC, Curran ME, Spector PS and Keating MT: Spectrum of HERG K+-channel dysfunction in an inherited cardiac arrhythmia. Proc Natl Acad Sci USA 93: 2208-2212, 1996.
33. Furutani M, Trudeau MC, Hagiwara N, Seki A, Gong Q, Zhou Z, Imamura S, Nagashima H, Kasanuki H, Takao A, *et al*: Novel mechanism associated with an inherited cardiac arrhythmia: Defective protein trafficking by the mutant HERG (G601S) potassium channel. Circulation 99: 2290-2294, 1999.
34. Paulussen A, Yang P, Pangalos M, Verhasselt P, Marrannes R, Verfaille C, Vandenberk I, Crabbe R, Konings F, Luyten W and Armstrong M: Analysis of the human KCNH2(HERG) gene: Identification and characterization of a novel mutation Y667X associated with long QT syndrome and a non-pathological 9bp insertion. Hum Mutat 15: 483, 2000.
35. Gong QM, Keeney DR, Robinson JC and Zhou ZF: Defective assembly and trafficking of mutant HERG channels with C-terminal truncations in long QT syndrome. J Mol Cell Cardiol 37: 1225-1233, 2004.